ASIAN JOURNAL OF CIVIL ENGINEERING (BUILDING AND HOUSING) VOL. 10, NO. 2 (2009)
PAGES 183-200

DEVELOPING SEISMIC FRAGILITY FUNCTION OF STRUCTURES BY STOCHASTIC APPROACH

K. Nasserasadi[*a], M. Ghafory-Ashtiany[b], S. Eshghi[b] and M.R. Zolfaghari[c]
[a] *Department of Civil, Faculty of Enginnering, Zanjan University, Zanjan, Iran*
[b]*International Institute of Earthquake Engineering and Seismology, Tehran, Iran*
[c]*Department of Civil Engineering, Khajenasir Toosi University, Tehran, Iran*

Abstract

Fragility function of structures is the major requirement of seismic loss estimation which is widely used in the seismic risk management. In this paper, firstly, a comprehensive and simplifies stochastic methods are presented for development of analytical fragility functions. Secondly, the effect of damage threshold uncertainty on fragility functions is estimated. It is shown that the results of the method are almost comparable with the result of previous studies and the effect of uncertainty of damage state on the deviation of fragility function in the lower intensity of ground motion is high which gradually decreases.

Keywords: Stochastic method; fragility function; fragility dispersion; vulnerability of structures; non-structural damage; hazus

1. Introduction

Evaluation of seismic fragility functions of structural which defines the probability of physical damage as a function of ground motion intensity parameter has gained importance recently due to its key rule in seismic loss assessment and risk management. Although some well-known fragility databases such as ATC-13 [2] and HAZUS [9] are available, these fragility functions are developed for general types of structures with substantial amount of assumptions and uncertainties. Due to wide usage of fragility functions in the next generation of seismic design codes [18], need for development of structure-specific fragility functions has increased. To answer to such demand, in this paper, a full stochastic method with a proposed simplified procedure is introduced.

Fragility and vulnerability functions are developed in three main ways: expert opinion, analytical methods and damage data of structures from past events [19]. Evaluation of fragility curves using existing data of earthquake damage is perhaps the best way to estimate potential damage of future earthquake which is used for fragility functions development in several studies [20,22,16,21]. In the absence of past damage data, the fragility functions are

[*] Email-address of the corresponding author: naserasadi@znu.ac.ir (K. Nasserasadi)

developed based on the opinion of experts. ATC-13 is a good example of such approach [2]. Nevertheless, when appropriate analytical tools are available, the analytical method is the right and proper method for fragility curve development of engineering and special structures.

Two general approaches have been utilized in development of analytical fragility functions: comparing capacity and demand of structures [e.g. 22, 23 and 6] and match up damage index to damage thresholds [e.g. 10, 25, 11 and 12]. Results of the first approach are more suitable for design purposes [3] while the results of the second methodology is more appropriate for the loss estimation purposes due to its ability to define damage states.

Stochastic methods by the means of Monte-Carlo simulation and artificial earthquake records generation have been employed for fragility functions [10, 24, 11 and 12]. However, due to existing uncertainties in these methods, demand for a straight-forward and rapid procedure of structure-specific fragility function calculation is still existed.

2. Definition of Fragility Function and Estimation Method

Due to practical reasons, continuous damage in structures is divided into several discrete damage states [19]. Fragility function estimates the conditional exceeding probability of damage from a damage state at given ground motion intensity:

$$F_i(im) = P(D > d_i \mid IM = im) \tag{1}$$

Where, $F_i\ (im)$ is the probability of exceeding damage "D" from damage state "d_i" at given ground motion "*IM=im*". Ground motion intensity parameters denotes the magnitude of ground motion which is measured by Peak Ground Acceleration (PGA), Peak Ground Velocity (PGV) or Spectral Displacement (SD) . Damage states "*i*" are defined from the non-damage state (i=0) to the n^{th} damage state (i=n) by qualitative and analytical definitions [see 9]. Since damage in structures, in this study, is measured by Damage Index (DI), Eq. (1) is changed to:

$$F_i(im) = P(DI > di_t \mid IM = im) \tag{2}$$

Where, di_t is the damage index at the threshold of damage states. Having the Probability Density function of "*DI*" or its cumulative distribution function at every *"im"* ($f_{im}(di)$ and $F_{im}(di_t)$), Eq. (2) is evaluated from probabilistic theorem:

$$F_t(im) = P(DI > di_t \mid IM = im) = 1 - F_{im}(di_t) = 1 - \int_{-\infty}^{di_t} f_{im}(di)d(di) \tag{3}$$

In this paper, PDF of DI is evaluated by multi-stripe analysis [1,8]. Here, structure is analyzed subjected to several real ground motion records that are all scaled to specific *IM* level and distribution of structural response in the particular *IM* is estimated from the results of the nonlinear analysis set.

Based on these assumptions, procedure of fragility curve development for real structure(s) is summarized in five major steps shown in flowchart of methodology given in Figure 1:

1. Selecting structure(s) with similar structural category and/or behavior.
2. Choosing a damage index and ground motion intensity measurement.
3. Selecting group of time history records and scaling them to selected IMs values. The selected records should represent the randomness of ground motion.
4. Estimating the distribution of damage index at the selected IMs through multi-stripe analyses and fitting proper distribution function to the results.
5. Calculating fragility values Using Eq. (3) and fitting appropriate function to the results.

Implementation of the above procedure is illustrated in the following example.

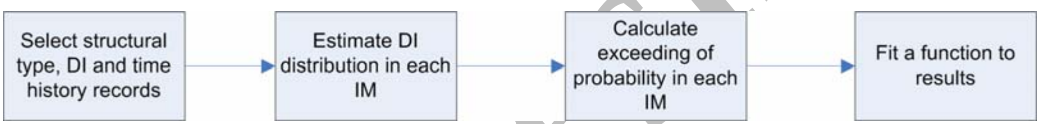

Figure 1. Procedure of estimating analytical fragility function

3. Illustrative Example

Two groups of low-rise steel frame which are compatible with high-code and moderate-code structural classifications of HAZUS were selected [9]. According to HAZUS, high-code frame corresponds to ductile steel structures designed for 0.133 fraction of building weight and moderate-code frame corresponds to semi-ductile steel frames which is designed for 0.067 fraction of building weight. For each classification, two low-rise steel moment resisting frames (two bay; two and three story) which are selected from a middle frame in a hypothetical building were designed. The elevation views of the frames are shown in Figure 2.

Following assumptions were made for fragility curve development:

- Spectral Displacement (SD) is chosen as *IM*.
- ISD is selected for damage index, due to its good representation of damage for structural and most of non-structural elements [19].
- Mean damage thresholds of HAZUS shown in Table 1 are chosen as medium threshold of damage states [9].

Table 1. Inter-story drift ration at thresholds of different damages states [9]

Seismic design level	Drift ration at threshold of structural damages			
	Slight	**Moderate**	**Extensive**	**Complete**
High-code	0.006	0.012	0.03	0.08
Moderate-code	0.006	0.0104	0.0235	0.06

For estimation *ISD* distribution in each ground motion value, a set of 20 records with a uniform distribution of source-to-site at a minimum distance of 10km to reduce the near source effect were selected from the PEER ground motion database (see Table 2) [17]. The distribution of source-to-site distance with the magnitude of selected records is shown in Figure 3. The records are scaled so that the 5% damped Spectral Displacement of records at the period of structures (0.13 and 0.149 for moderate and high code) equals to 2.5, 5, 10, 20, 30, 40, 50, 60, 70, 80 and 90cm. Structures were analyzed by OPENSEES [15] subjected to scaled records. P-Δ effect were considered and FEMA-356 force-deformation relationship [7] was selected for plastic hinge property of the structural elements.

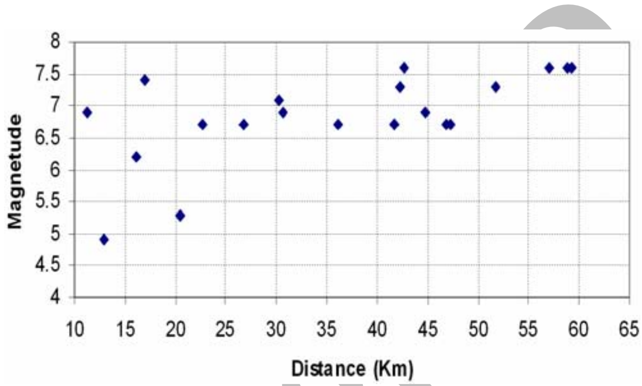

Figure 3. Distribution of distance and magnitude of selected records

Table 2. Selected strong motion records for non-linear dynamic analysis [17]

ID	EQ name	Date and time of earthquake	Epicenter Distance	M
1	Loma Prieta	1989/10/18 00:05	11.2	6.9
2	Anza (Horse Cany)	1980/02/25 10:47	13	4.9
3	Kocaeli, Turkey	1999/08/17	17	7.4
4	Morgan Hill	1984/04/24 21:15	16.2	6.2
5	Whittier Narrows	1987/10/04 10:59	20.4	5.3
6	Northridge	1994/01/17 12:31	22.7	6.7
7	Loma Prieta	1989/10/18 00:05	30.6	6.9
8	Northridge	1994/01/17 12:31	26.8	6.7
9	Duzce, Turkey	1999/11/12	30.2	7.1
10	Chi-Chi, Taiwan	1999/09/20	42.7	7.6
11	Northridge	1994/01/17 12:31	36.1	6.7
12	Northridge	1994/01/17 12:31	41.7	6.7
13	Landers	1992/06/28 11:58	42.2	7.3
14	Loma Prieta	1989/10/18 00:05	44.8	6.9
15	Northridge	1994/01/17 12:31	47.3	6.7
16	Northridge	1994/01/17 12:31	46.9	6.7
17	Chi-Chi, Taiwan	1999/09/20	57.06	7.6
18	Landers	1992/06/28 11:58	51.7	7.3
19	Chi-Chi, Taiwan	1999/09/20	58.8	7.6
20	Chi-Chi, Taiwan	1999/09/20	59.26	7.6

The distribution of maximum *ISD* which is estimated from the analyses of moderate and high code structures are shown in Figures 4 and 5 where the mean thresholds of damage states from Table 1 are shown as well. To find appropriate distribution function for ISDs, normal and log-normal distribution functions were tested. Although lognormal distribution rather inappropriate for higher level of *SD*s especially in the moderate code frames, it was better fitted to *ISD* distributions in general. Mean and lognormal deviation ($I\hat{S}D_{sd}$ and β_{sd}) of *ISD* distributions of high-code frames are shown in Table 3.

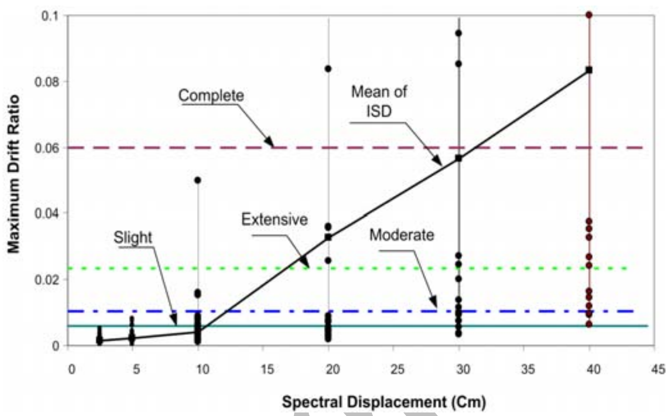

Figure 4. Maximum ISD of moderate code design frames; horizontal lines are damage thresholds

Table 3. Mean and deviation values of log-normal distribution of ISD data in each SD for high code frame

SD (cm)	2.5	5	10	20	30	40	50	60	70	80	90
$I\hat{S}D_{sd}$	0.001	0.001	0.003	0.005	0.008	0.013	0.018	0.020	0.106	0.139	0.185
β_{sd}	0.778	0.771	0.682	0.702	0.853	1.062	1.106	1.192	1.281	0.973	1.561

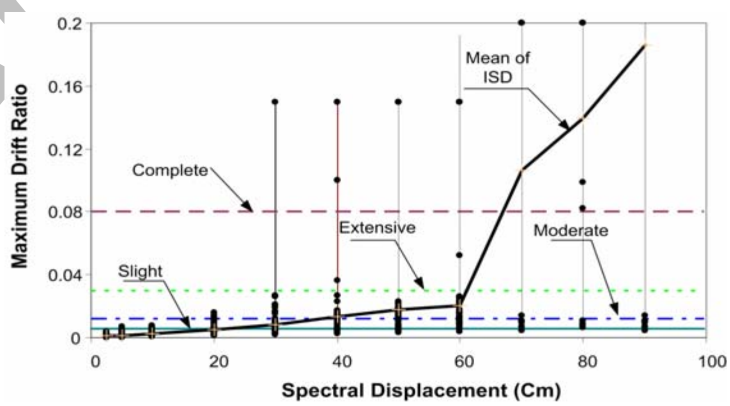

Figure 5. Maximum ISD of high code design frames; horizontal lines are damage thresholds

The fragility value at each sd ($F_i(sd)$) is estimated by changing the notation of Eq. (3) and replacing the distribution of damage index ($f_{im}(di)$) by lognormal distribution of ISD ($f(isd) = \phi[\ln(\hat{ISD}_{sd}), \beta_{sd}]$):

$$F_i(sd) = P(D > d_i \mid SD = sd) = 1 - P(D \le d_i \mid SD = sd) = 1 - \Phi(1/\beta_{sd} . \ln(ISD_i / \hat{ISD}_{sd})) \quad (4)$$

Where, ISD_i is the mean ISD threshold of damage states (e.g. Table 1). The results for the moderate and high code frames are shown in Figures 6 and 7 by dots. Fragility functions shown in the figures are estimated by fitting a log-normal cumulative distribution function:

$$F_i(sd) = P(D > d_i \mid SD = sd) = \Phi(\frac{1}{\beta_i} \ln(\frac{sd}{SD_i})) \quad (5)$$

Where SD_i and $\boldsymbol{\beta}_i$ are mean and deviation of the function respectively. These parameters for the fragility functions are given in Table 4.

Table 4. Parameters of fragility functions estimated from comprehensive procedure

Code design level	Slight		Moderate		Extensive		Complete	
	SD$_m$ (cm)	**B**	**SD$_m$ (cm)**	**β**	**SD$_m$ (cm)**	**β**	**SD$_m$ (cm)**	**β**
Moderate code	11	0.62	16	0.42	20	0.5	30.12	0.67
High code	26	0.57	37	0.52	55	0.33	69	0.35

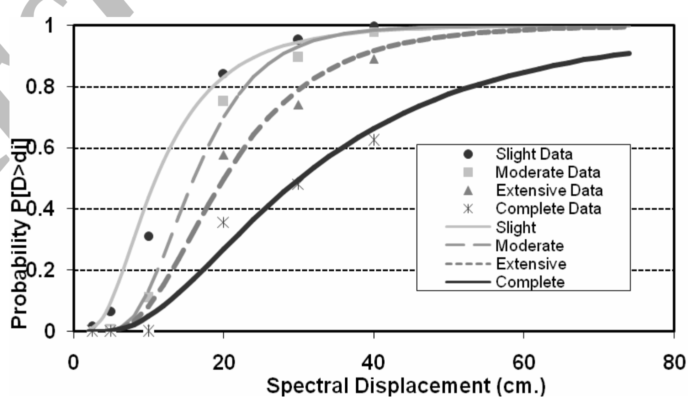

Figure 6. Fragility values and functions for moderated code design steel moment resistant frame

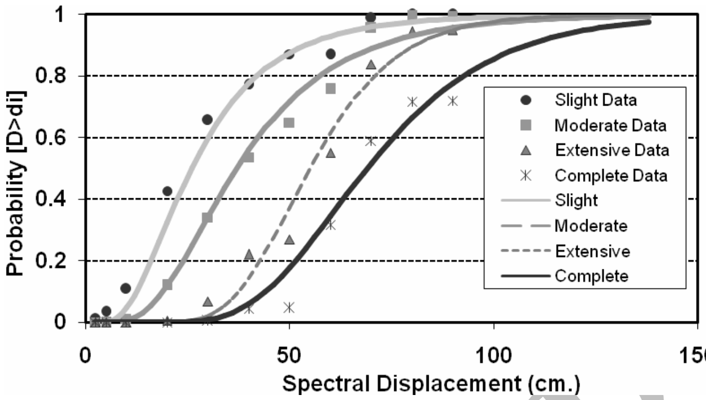

Figure 7. Fragility values and functions for high code design steel moment resistant frame

4. Non-Structural Damage Governing Case

Most direct and indirect loses stem from damage to non-structural elements and evaluation of damage probability to these elements is important in the most of the cases. The proposed method provides a useful tool for evaluation of fragility functions when non-structural elements govern the damage states. For instance, damage to mounted equipment in industrial facilities is one of the damage conditions of supporting structures. Since damage to most of non-structural damages are defined by ISD [19], the corresponding fragility function can be estimated by replacing the related ISD as damage threshold (ISD_i) in Eq. (4). These thresholds can be estimated from experimental studies or working condition of equipments.

For instance, in the illustrative example, two additional damage states are defined to determine the pipe leakage and damage to equipment supports with associated ISD of 0.0033 and 0.0083 respectively. The resulted fragility functions which are shown in Figure 8 can be used to evaluate the probability of relative non-structural damages.

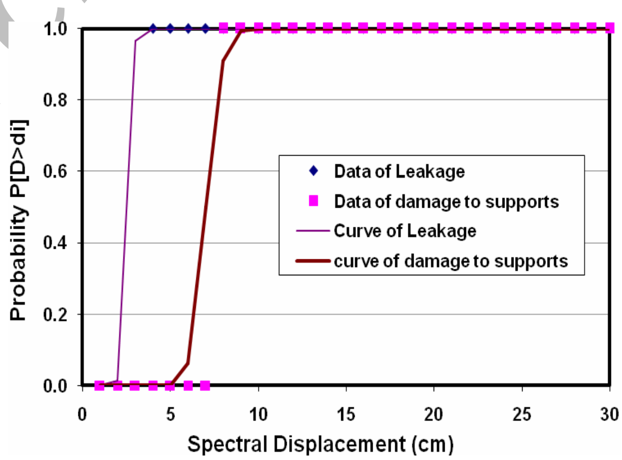

(a) High code

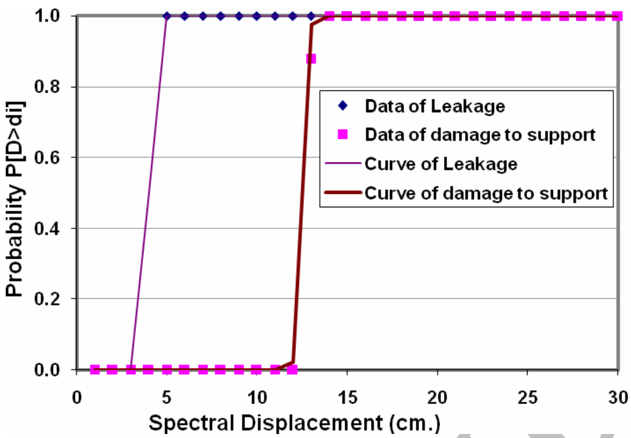

(b) Moderate code

Figure 8. Fragility function result for equipment governing damage state :probability of leakage in the pipes and damage to equipment support

5. Effect of Uncertainty of Damage Thresholds

Thresholds of damage states are not a sharp limit, but they are defined by a distribution of damage threshold. According to existing literature, lognormal distribution has been used for that [9,27]:

$$ISD = ISD_i.\varepsilon_{t(i)} \tag{6}$$

Where, ISD_i is the mean *ISD* threshold at damage state "*i*",(e.g. Table 1) and $\varepsilon_{t(i)}$ is a random variable with log-normal distribution, mean of unit and deviation of $\beta_{t(i)}$.

The effect of this uncertainty on fragility functions can be quantified by fragility dispersion. So far the mean value of fragility function at every ground motion is estimated by using the mean value of damage threshold in Eq. (5) (i.e. ISD_i). By the same token, if the dispersion of damage threshold from Eq. (6) is utilized in Eq. (5) the distribution of fragility value or fragility deviation at every ground motion is calculated:

$$F_i(sd) = 1 - \Phi(1/\beta_{sd}.\ln(ISD_i.\varepsilon_{t(i)} / \hat{ISD}_{sd})) \tag{7}$$

Eq. (7) is solved by Monte-Carlos simulation for $\beta_{t(i=1..4)} = 0.4$, as suggested by HAZUS [9], for all fragility function in the illustrative example and the distribution of fragility value is estimated at every *sd*. Deviation of fragility function ($\beta_t(sd)$) is estimated by fitting log-normal distribution, which is more proper compare to normal distribution based on examination, to the fragility distribution at every *sd*. Figure 9 has shown variation of $\beta_t(sd)$ vs. *sd* for the fragility functions shown in Figures 6 and 7.

From Figure 9 it can be observed that the deviation of fragility function is high in the lower IMs and could reach to 3.5 times of damage threshold deviation (i.e. $\beta_{t(i=1..4)} = 0.4$).It gradually decreases by increasing of IMs.

6. Simplified Method for Developing Fragility Function

The proposed method derives the damage index distribution through substantial number of non-linear dynamic analyses which is expensive and inconvenient for most of practical applications. A rapid method of fragility function development is introduced by taking advantage of recent development in estimation of structural capacity by converting push-over (SPO) curve of structures to distribution of incremental dynamic curves [26] which is very similar to ISD distribution.

The necessary steps for fast derivation of ISD distribution based on modified flowchart shown in Figure 10 are:

1. Converting SPO curve of structure from "*top displacement-base share*" space to *R-μ* space by dividing the horizontal axis of the diagram by Δ_y and the vertical axis by V_y .

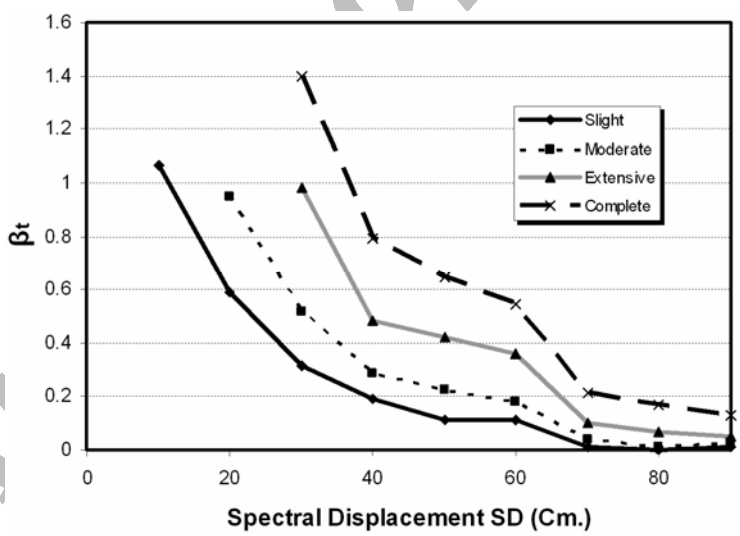

(a) High code structure

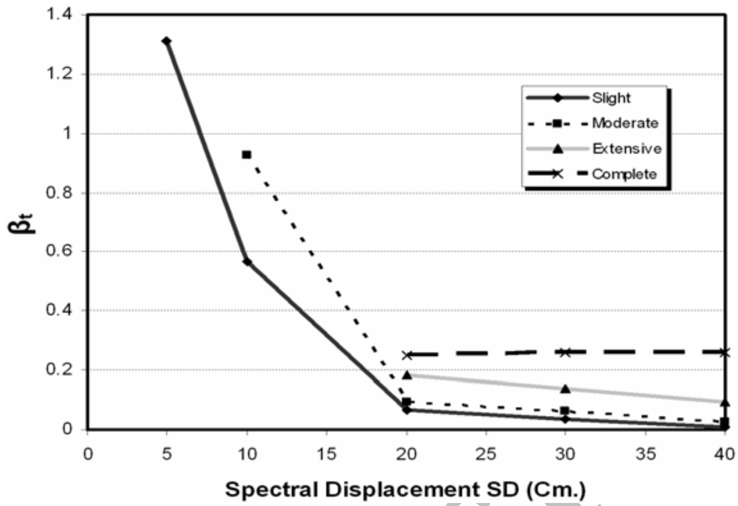

(b) Moderate code structure

Figure 9. Deviation of fragility function dispersion (β_t) as a function of SD

2. Generating the set of IDA curves in *R-μ* space using SPO2IDA software which is available online [26].
3. Converting IDA curves from R-μ space to *SD-ISD* space by multiplying the horizontal axis by $\theta_{\max y}$ and vertical axis by $g.S_{a_y}/\omega^2$.

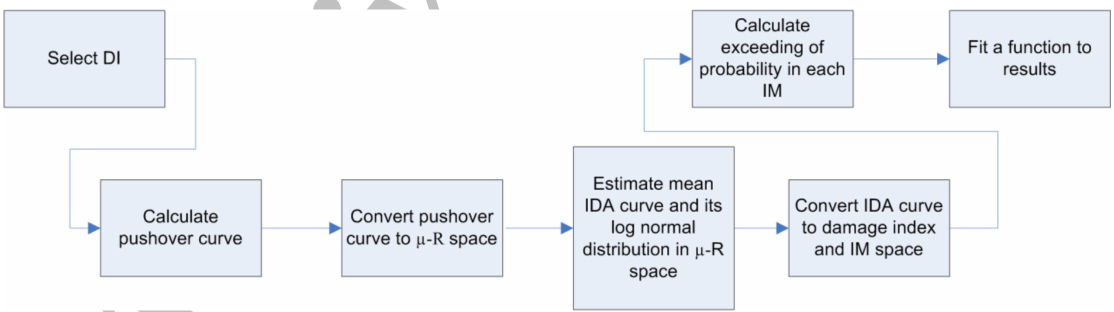

Figure 10. Flowchart of simplified method of fragility function estimation

The simplified method was applied to 3-story structures of the examples shown in Figure 2. Pushover diagrams of these structures and its converted diagram are shown in Figure 11. The IDA curve in R-μ space estimated by SPO2IDA software and converted to *SD-ISD* are given in Figure 12. For comparison, the results of non-linear dynamic analyses are shown in the figure as well.

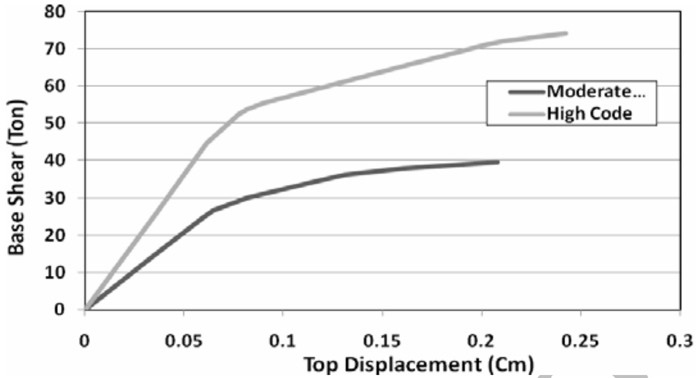

(a) Base-shear vs. Displacement

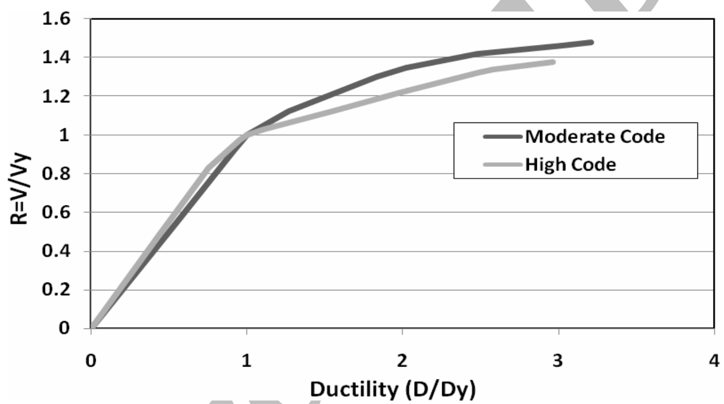

(b) Over strength vs. Ductility

Figure 11. Pushover curves for high code and moderate code structures

Fragility value at each *IM* is estimated by applying Eq. (4) to new *ISD* distribution at each *SD*. In the equation, $\hat{ISD}_{sd}$ is directly estimated from the 50% IDA curve ($x_{50\%}$) and β_{SD} is estimated from and 16% or 84% IDA curves at each *IM* ($x_{16\%}$ and $x_{84\%}$):

$$\beta_{sd} = \ln(x_{16\%} / x_{50\%}) / \Phi^{-1}(0.16) = \ln(x_{84\%} / x_{50\%}) / \Phi^{-1}(0.84) \tag{8}$$

Fragility value and functions are shown in Figure 13. The parameters of fragility function are given in Table 5.

Table 5. Parameters of fragility functions estimated from simplified procedure

Code design level	Slight		Moderate		Extensive		Complete	
	SD_m (cm)	β	SD_m (cm)	β	SD_m (cm)	β	SD_m (cm)	β
Moderate code	4	0.2	12	0.11	30	0.185	40	0.1
High code	10	0.02	19	0.02	53	0.2	73	0.1

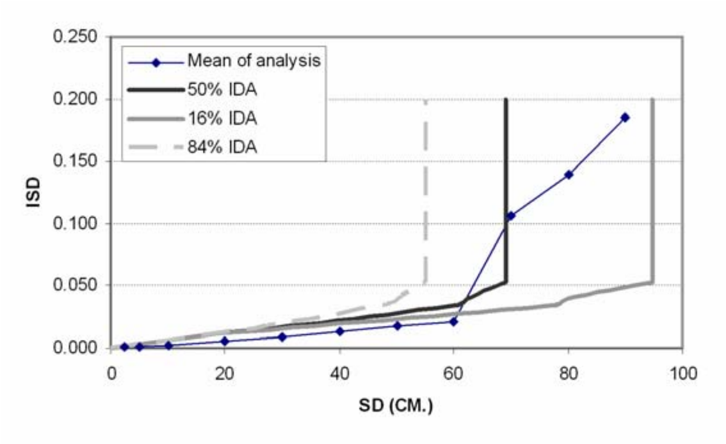

(a) High code IDA

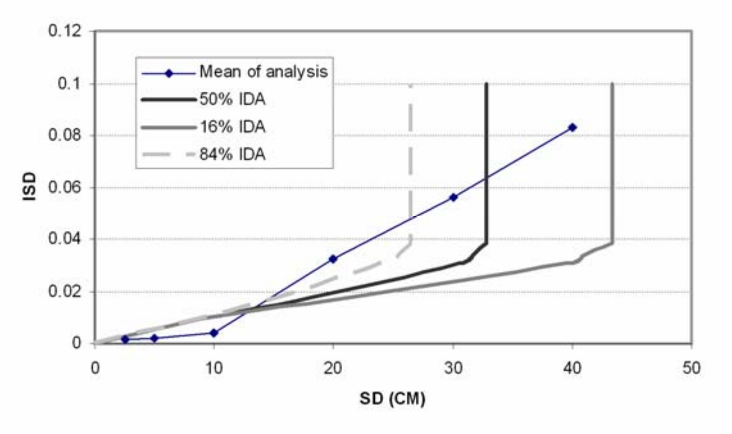

(b) Moderate code IDA

Figure 1. Converted IDA curve for high code and moderate code structures to SD-ISD space

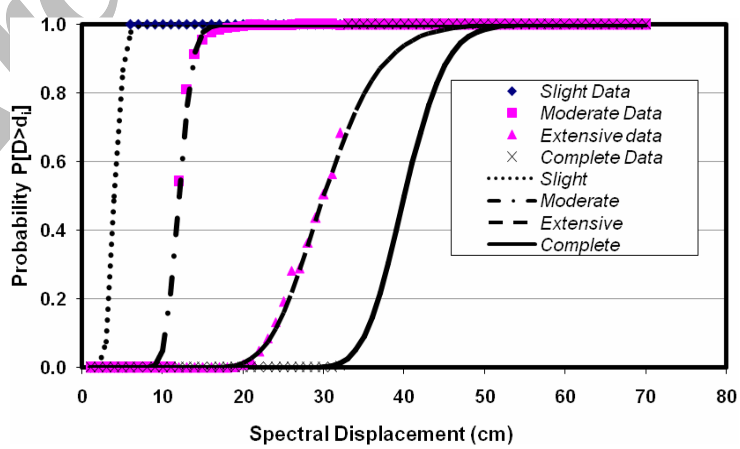

(a) High code

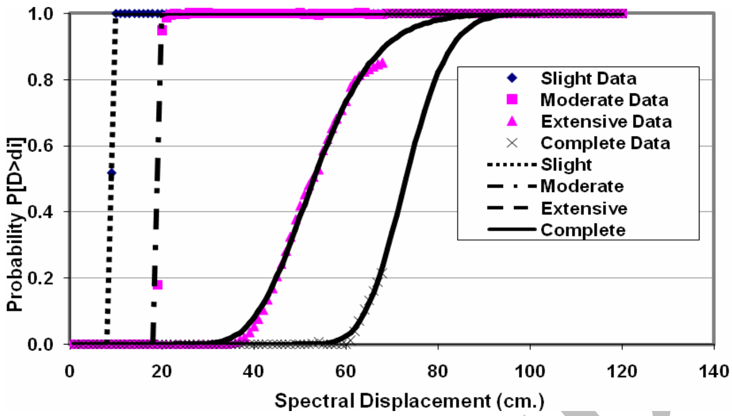

(b) Moderate code

Figure 13. Fragility function result of simplified method

7. Validation and Conclusions

In this paper, full and simplified methods for seismic fragility function development of structures are introduced. In addition, application of the method in development of non-structural governing damages is shown and effect of damage threshold uncertainty on fragility dispersion is estimated.

The result of full and rapid method for high and medium code design frames are compared with fragility of ductile [3 and 5] and semi-ductile [25] low-rise steel frames presented in Figure 14 and Figure 15. It can be observed that in the first place, the results of full and simplified method are very close in the extensive and complete damage states and in the second place, the results of the method are almost comparable with the results of previous studies.

To sum up, development of structure-specific fragility function is the key elements of accurate risk assessment. In this paper, full and rapid methods for derivation of structure-specific fragility functions are introduced. It is observed that, the results of the method are almost comparable with the previous studies and the effect of uncertainty of damage state on the deviation of fragility function in the lower intensity of ground motion is high which gradually decreases.

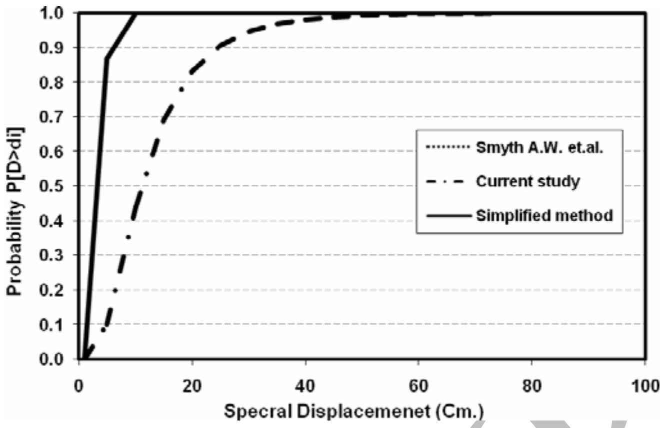

(a) Slight damage state

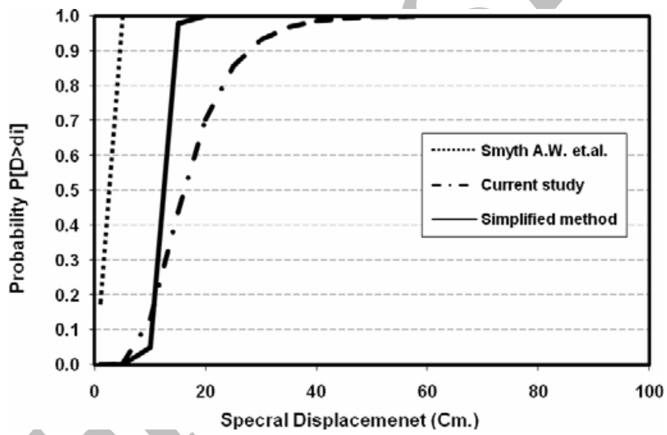

(b) Moderate damage state

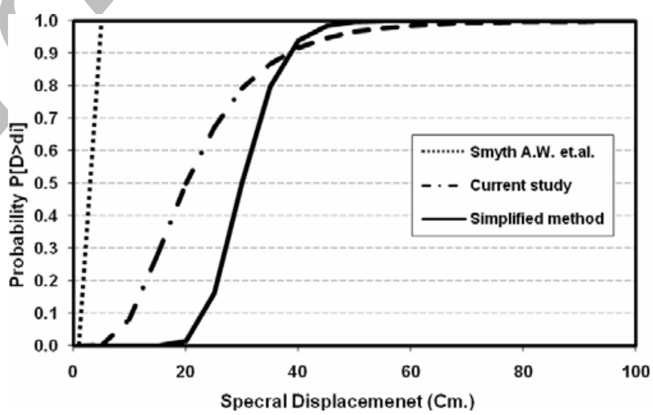

(c) Extensive damage state

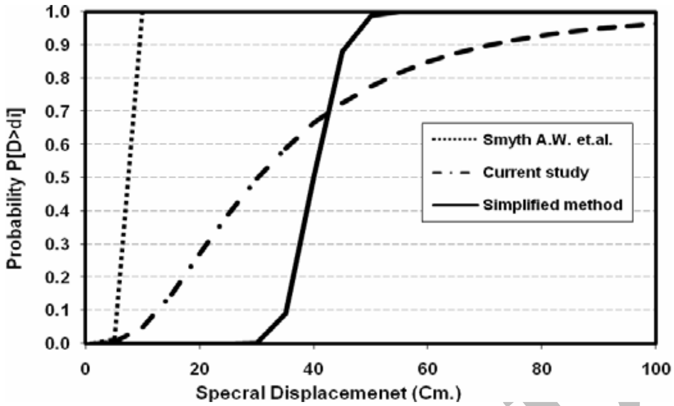

(d) Complete damage state

Figure 14. Comparison of fragility functions for moderate code steel frame structure

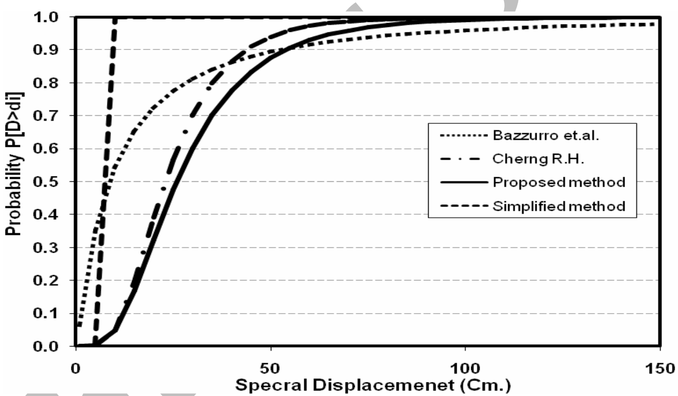

(a) Slight damage state

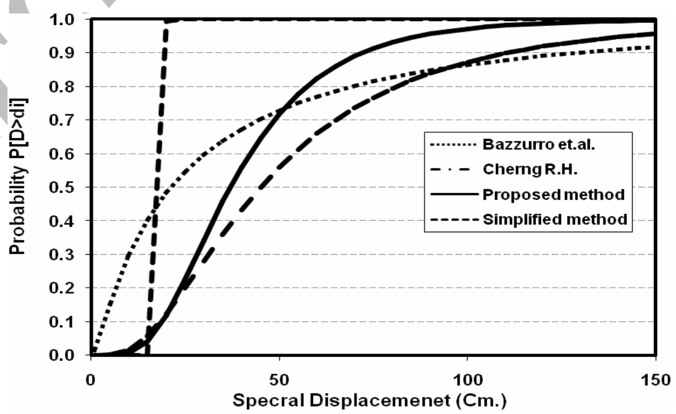

(b) Moderate damage state

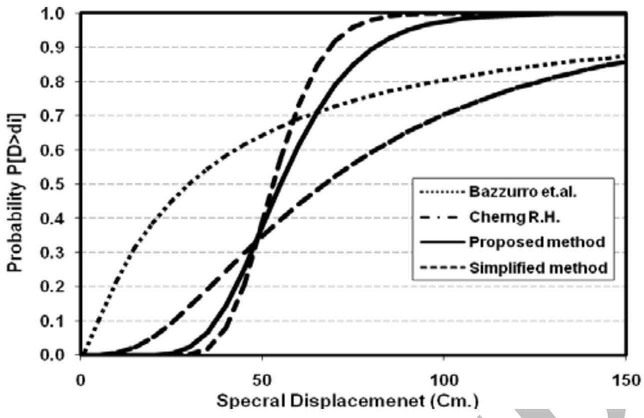

(c) Extensive damage state

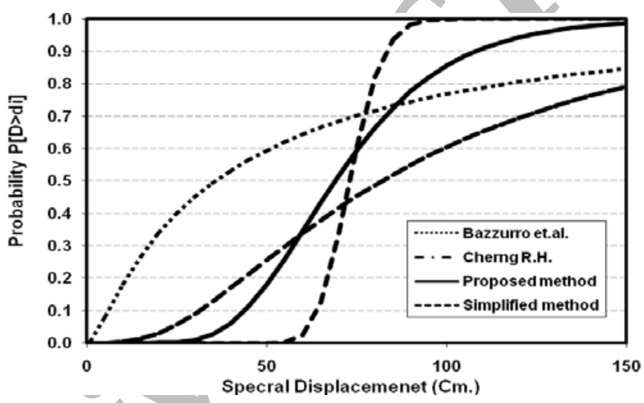

(d) Complete damage state

Figure 15. Comparison of fragility functions for high code steel frame structure

References

1. Aslani H, Miranda E. Optimization of response simulation for loss estimation using PEER's methodology, *Proceeding of the 13th World Conference on Earthquake Engineering*, Vancouver, Canada, Paper No. 1066, 2004.
2. ATC, *Earthquake damage evaluation data for California*, American Technology Council Report. No. 13, 1985.
3. Bazzurro P, Cornell CA, Menun C, Luco N, Motahari M. *Advanced seismic assessment guidelines*, Report for Pacific Gas and Electric/PEER Lifelines Program, Task 507, 2004.
4. Chambers JM *Graphical methods for data analysis*, Chapman and Hall, 1983.
5. Cherng RH. Preliminary study on the fragility curves for steel structures in Taipei, *Earthquake Engineering and Engineering Seismology,* **3**(2000)135-42.
6. Dimova Sl, Hirata K. Simplified seismic fragility analysis of structures with two types of

friction devices, *Journal of Earthquake Engineering And Structural Dynamics*, **29** (2000)1153-75.

7. FEMA-356, *Prestandard and Commentary For The Seismic Rehabilitation of Buildings*, Federal Emergency Management Agency (FEMA), Doc. No. 356, 2000.
8. Jalayer F. Direct probabilistic seismic analysis: implementing non-linear dynamic assessments, PhD thesis Civil and Environmental Engineering Department, University Stanford, California, 2003.
9. HAZUS.*Earthquake loss estimation methodology-Technical manual*, Federal Emergency Management Agency and National Institute of Building Science, 1999.
10. Hwang HHM, Huo J-w. Generation of hazard-consistent Fragility curves, *Journal of Soil Dynamic and Earthquake Engineering*, **13**(1994)345-54.
11. Karim KR, Yamazaki F. Effect of Earthquake Ground Motions on Fragility curves of highway bridge piers based on numerical simulation, *Journal of Earthquake Engineering and Structural Dynamics* , **30**(2001)1839-56.
12. Karim KR, Yamazaki F. A simplified method of constructing fragility curves for highway bridges, *Journal of Earthquake Engineering and Structural Dynamics*, **32**(2003) 1603-26.
13. Kennedy RP, Cornell CA, Campbell RD. Probabilistic seismic safety study of an existing nuclear power plant, *Journal of Nuclear Engineering and Design*, No. 2, **59**(1980)315-38.
14. Kwon OS, Elnashai A. The effect of material and ground motion uncertainty on the seismic vulnerability curves of RC structures, *Journal of Engineering Structures*, **28** (2006)289-303.
15. Open Sees, *Open System for Earthquake Engineering Simulation*, http://opensees.berkeley.edu/index.php, 2006.
16. O'Rourke MJ, So P. Seismic fragility function for on-grade steel tanks, *Earthquake Spectra*, No. 4, **16**(2000)1167-83.
17. Pacific Earthquake Engineering Research center (PEER) online strong motion database, http://peer.berkeley.edu/smcat/.
18. Porter K, Kennedy R, Bachman R. Derivation and use of fragility functions in performance-based earthquake engineering, *Earthquake Spectra*, No. 1, **22**(2007)
19. Porter KA. Assembly-based vulnerability of buildings and its use in seismic performance evaluation and risk-management decision-making, PhD thesis Civil and Environmental Engineering Department , University Stanford, California, 2000.
20. Sabbetta F, Goretti A, Lucantoni A. Empirical Fragility Functions From Damage Surveys And Estimated Strong Ground Motion, *Proceeding of the 11th European Conference on Earthquake Engineering*, Paris, 1998.
21. Sarabandari P, Pachakis D, King S, Kiremidjian S. Empirical Fragility Functions From Recent Earthquakes, *Proceeding of the 13th World Conference on Earthquake Engineering*, Vancouver, Canada Paper No. 1211, 2004.
22. Shinozoka M, Feng MQ, Lee J, Naganuma T. Statically analysis of fragility functions, *Journal of Engineering mechanics, ASCE* , No. 12, **126**(2000)1224-31.
23. Shinozoka M, Feng MQ,Kim HK, Kim SH. Nonlinear Static Procedure for fragility function Development, *Journal of Engineering Mechanics, ASCE,* No. 12, **126**(2000)

1287-95.
24. Singhal A, Kiremidjian S. Method for probabilistic evaluation of seismic structural damage, *Journal Of Structural Engineering, ASCE*, No. 12, **122**(1996)1459-67.
25. Smyth AW, Deodatis G, Franco G, He Y, Gurvich T. Evaluating Earthquake Retrofitting Measures For Schools: A Demonstration Of Cost-Benefit Analysis, Department of Civil Engineering and Engineering Mechanic, Columbia University, New York, 2004.
26. Vamvatsikos D, Cornell CA. Direct estimation of seismic demand and capacity of multi degree-of-freedom systems through incremental dynamic analysis of single degree of freedom approximation, *Structural Engineering*, No .4, **131**(2005)589-99.
27. Wen YK, Ellingwood BR, Veneziano D, Bracci J. *Uncertainty Modeling In Earthquake Engineering*. MAE Center Project, Report FD-2, 2003.